9. Voilmer, R. & Norry, M. J. *Nature* **301,** 141–143 (1983).
10. Hawkesworth, C. J., Kempton, P. D., Rogers, N. W., Ellam, R. M. & van Calsteren, P. W. *Earth planet. Sci. Lett.* **96,** 256–268 (1990).
11. Hart, S. R. *Nature* **309,** 753–757 (1984).
12. Sun, S.-S. & McDonough, W. F. in *Magmatism in the Ocean Basins* (ed. Saunders, A. D. & Norry, M. J.) 313–345 (Geol. Soc. Spec. Publ. No. 42, Blackwell Scientific, Oxford, 1989).
13. Davies, G. R., Norry, M. J., Gerlach, D. C. & Cliff, R. A. in *Magmatism in the Ocean Basins* (ed. Saunders, A. D. & Norry, M. J.) 231–255 (Geol. Soc. Spec. Publ. No. 42, Blackwell Scientific, Oxford, 1989).
14. Halliday, A. N., Dickin, A. P., Fallick, A. E. & Fitton, J. G. *J. Petrol.* **29,** 181–211 (1988).
15. Gerlach, D. C., Cliff, R. A., Davies, G. R., Norry, M. & Hodgson, N. *Geochim. cosmochim. Acta* **52,** 2979–2992 (1988).
16. Newsom, H. E., White, W. M., Jochum, K. P. & Hofmann, A. W. *Earth planet. Sci. Lett.* **80,** 299–313 (1986).
17. Ito, E., White, W. M. & Gopel, C. *Chem. Geol.* **62,** 157–176 (1987).
18. Palacz, Z. A. & Saunders, A. D. *Earth planet. Sci. Lett.* **79,** 270–280 (1986).
19. White, W. M. & Hofmann, A. W. *Nature* **196,** 821–825 (1982).
20. Gerlach, D. C., Stormer, J. C. Jr & Mueller, P. A. *Earth planet. Sci. Lett.* **85,** 129–144 (1987).
21. Mitchell-Thomé, R. G. *Geology of the South Atlantic Islands* (Gebrüder Borntraeger, Berlin, 1970).
22. Mitchell-Thomé, R. G. *Geology of the Middle Atlantic Islands* (Gebrüder Borntraeger, Berlin 1976).
23. Hughes, D. J. & Brown, G. C. *Contrib. Mineral. Petrol.* **37,** 91–109 (1972).
24. Fitton, J. G. & Dunlop, H. M. *Earth planet. Sci. Lett.* **72,** 23–38 (1985).
25. Seitz, M. G. *Yb Carnegie Instn Wash.* **72,** 551–553 (1973).
26. Watson, E. B., Ben Othman, D., Luck, J.-M. & Hoffmann, A. W. *Chem. Geol.* **62,** 191–208 (1987).
27. McKenzie, D. & O'Nions, R. K. *J. Petrol.* **32,** 1021–1091 (1991).
28. Jochum, K. P., Hofmann, A. W., Ito, E., Seufert, H. M. & White, W. M. *Nature* **306,** 431–436 (1984).
29. Hofmann, A. W., Jochum, K. P., Seufert, M. & White, W. M. *Earth planet Sci. Lett.* **79,** 33–45 (1986).
30. Wyllie, P. J. *J. geophys. Res.* **93,** 4171–4181 (1988).
31. McKenzie, D. *Earth planet. Sci. Lett.* **74,** 81–91 (1985).
32. McKenzie, D. *Earth planet. Sci. Lett.* **72,** 149–157 (1985).
33. Fielding, K. D., Fitton, J. G., Ford, C. E. & Hinton, R. W. *Terra Abstr.* **3,** 419 (1991).
34. Schneider, M. E. & Eggler, D. H. *Geochim. Cosmochim. Acta* **50,** 711–724 (1986).
35. Watson, E. B., Brennan, J. M. & Baker, D. R. in *Continental Mantle* (ed. Menzies, M.) 111–124 (Clarendon, Oxford, 1990).
36. Michael, P. J. *Geochim. cosmochim. Acta* **52,** 555–566 (1988).
37. Richards, M. A. & Griffiths, R. W. *Nature* **342,** 900–902 (1989).
38. Sano, Y., Wakita, H., Ohsumi, T. & Kusakabe, M. *Geophys. Res. Lett.* **14,** 1039–1041 (1987).

ACKNOWLEDGEMENTS. We thank K. O'Nions, R. Lange and Y. Zhang for discussions, colleagues in the Radiogenic Isotope Geochemistry Laboratory for criticism of the text, and W. White for a review. The research was supported by NSF grants to A.N.H.

A sharp and flat section of the core–mantle boundary

John E. Vidale & Harley M. Benz

United States Geological Survey, Branch of Seismology,
345 Middlefield Road MS 977, Menlo Park, California 94025, USA

THE transition zone between the Earth's core and mantle plays an important role as a boundary layer for mantle and core convection[1]. This zone conducts a large amount of heat from the core to the mantle, and contains at least one thermal boundary layer[2,3]; the proximity of reactive silicates and molten iron leads to the possibility of zones of intermediate composition[4]. Here we investigate one region of the core–mantle boundary using seismic waves that are converted from shear to compressional waves by reflection at the boundary. The use of this phase (known as ScP), the large number of receiving stations, and the large aperture of our array all provide higher resolution than has previously been possible[5–7]. For the 350-km-long section of the core–mantle boundary under the northeast Pacific sampled by the reflections, the local boundary topography has an amplitude of less than 500 m, no sharp radial gradients exist in the 400 km above the boundary, and the mantle-to-core transition occurs over less than 1 km. The simplicity of the structure near and above the core–mantle boundary argues against chemical heterogeneity at the base of the mantle in this location.

The regional seismic networks of the United States and Canada routinely record local and distant earthquakes, mainly in order to monitor active faults within the networks. Together, these networks include more than 1,500 stations and span a wide aperture. This set of receivers is ideal for observing short-period seismic waves from distant earthquakes across larger distances than previously possible[8].

The phase ScP travels from the earthquake to the core–mantle boundary (CMB) as an S wave, then converts to a P wave for the remaining path to the receiver (Fig. 1*a*). ScP appears in a particularly quiet interval on seismograms for an earthquake that occurred on 13 March 1992, 180 km beneath the Andreanof Islands (magnitude m_b 6.1, 52.8° N, 178.8° W). We analyse seismograms from the University of Washington Seismic Network (125 stations), the Southern California Seismic Network (216 stations) and the Northern California Seismic Network (405 stations). The high signal-to-noise ratios of these seismograms will reveal the degree of lateral variation in structure near the CMB, the presence or absence of structure above the CMB and the sharpness of the CMB. These data are only sensitive to lateral variations in the CMB with wavelengths of 50 to 200 km, these limits arising from the limitations in resolution of 1-Hz seismic waves and the 15° aperture of the array, respectively. The data are sensitive to radial variations with wavelengths up to 10 km, beyond which insufficient short-period energy is reflected.

A smaller (m_b 5.3) event on 27 March 1992 (52.8° N, 174.0° W, 190 km depth) produced a particularly sharp set of arrivals, but was only available on the Northern California Seismic Network. The simplicity of the earthquake allows a direct measure of the simplicity of the CMB.

ScP is prominent in the distance range from 30° to 70° because the conversion coefficient at the CMB is large. The main source of short-period noise in this time interval is the coda of the P wave, which attenuates rapidly with time after the P wave passes. We study the CMB with the ScP phase rather than the more traditional choice of PcP[5–7] (Fig. 1) because ScP arrives 4 minutes later with a more favourable signal-to-noise ratio.

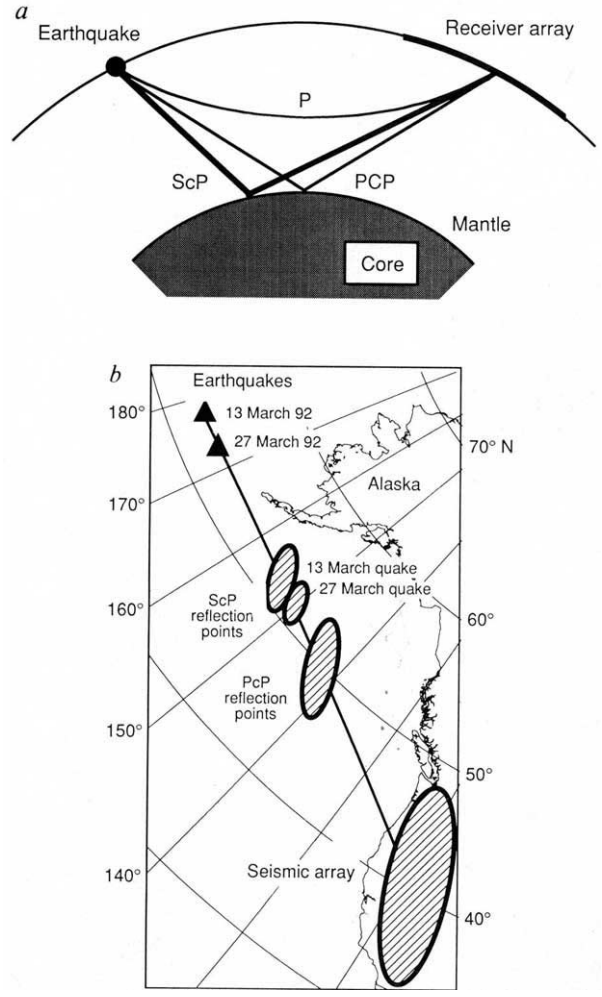

FIG. 1 Schematic ray paths (*a*) and bounce points at the core–mantle boundary (*b*) for the seismic waves analysed here.

We selected the ScP arrivals at the 362 out of 746 stations with the highest signal-to-noise ratio. These phases were aligned, then the seismograms were summed for 1° distance intervals (Fig. 2*a*), revealing nearly identical waveforms across the array. The ScP arrival lasts ~5 s, typical of the source duration for magnitude 6.1 earthquake. The complexity caused by the source duration is then removed by first estimating the source time function to be the sum of all the aligned traces, then deconvolving this sum from each trace. Deconvolved traces summed in 1° bins are shown in Fig. 2*b*. Again, the waveforms are nearly identical. The smaller earthquake, 400 km closer to the array and at a slightly different azimuth, is a more impulsive source (Fig. 2*c*). It samples a 130-km patch of the CMB adjacent to the 250-km patch sampled by the first earthquake. The waveform of the ScP phase does not vary across the array.

For the smaller earthquake, we aligned and summed the P waves, aligned and summed the ScP waves, and summed the PcP waves aligned according to ScP with the expected decrease in apparent velocity across the array (Fig. 3*a*). The ability to stack more than 100 seismograms eliminates the near-receiver crustal reverberations that have complicated previous comparisons of P with PcP[5,6]. Only the P and ScP arrivals contained enough energy in the interval 0.5 to 10 s to allow removal of the instrument response (Fig. 3*b*). The similarity of the P, PcP and ScP frequency content requires that the shear wave attenuation is low along the path from the earthquake to the CMB, which has also been observed for other paths[9].

Overall, the ScP, P and PcP waveforms are similar, particularly in the first second, indicating that the CMB is primarily a sharp transition. Our observations do not show differences as large as those that have been interpreted in noisier data as evidence for a laminated CMB[6].

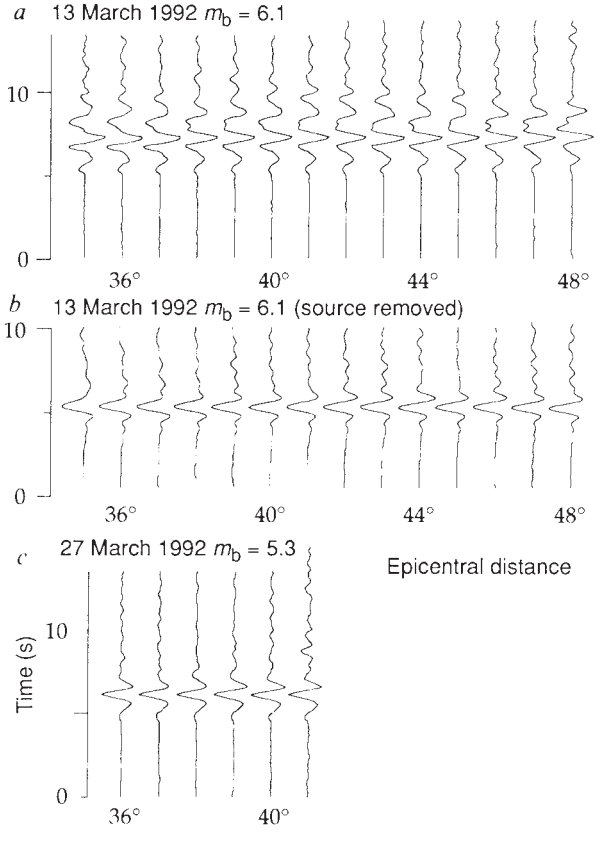

FIG. 2 Seismograms summed over 1° distance intervals are shown after alignment of the ScP phases for *a*, the 13 March 1992 Andreanof earthquake; *b*, deconvolved records of the 13 March 1992 Andreanof earthquake; and *c*, the 27 March Andreanof earthquake. These traces are from short-period, vertical-component seismograms that have usable signal from 0.5 to 10 s period for these earthquakes. The traces show the similarity of the ScP phases.

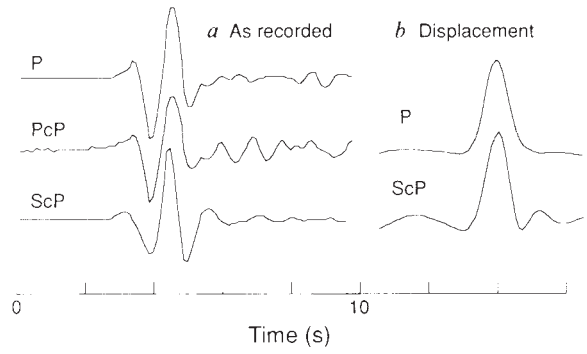

FIG. 3 *a*, Waveforms of the P, PcP and ScP waves of the 27 March 1992 earthquake (m_b = 5.3) estimated by the summation of 110–120 clean records from the Northern California Seismic Network. *b*, P and ScP displacement time histories. A 12-s period sine wave was added to cancel the long-period motions not resolved by our limited passband (see Fig. 2 legend).

The similarity of the waveforms in Figs 2 and 3 places tight limits on possible CMB topography. Calculations for a CMB with 500 m of relief[10,11] show resolvable waveform complexity that varies with epicentral distance and azimuth. Our observations therefore require less than 500 m topography with 50 to 200 km wavelength, although we can not preclude topography with larger or smaller scale. The small variations that are visible in the later half of the ScP waveform in Fig. 2*a* and *b* may arise from a few hundred metres of CMB topography or velocity variations above the CMB. Source directivity is a less likely explanation as the entire P-wave arrival is similar across the array, and a greater range of take-off angles is spanned by P than by ScP.

The P wave in Fig. 3*b* is very simple, showing that the earthquake lasted only 1 to 2 s. The ScP wave has one more half cycle than P and PcP in Fig. 3*a*, and this translates into the small secondary peak on the displacement record. The extra half cycle is visible for all bins in Fig. 2*c*. This complexity is difficult to attribute to extra attenuation of the S wave, because attenuation would cause the higher frequencies to arrive earlier, not later as observed. It is also difficult to attribute the complexity to lateral heterogeneity near the CMB, as a reflection from a point scatterer at or above the CMB should shift noticeably in time across the array. The difference may be due to a difference between the P- and S-wave radiation from the source.

Structures above the CMB would generate precursors to ScP. We expect structure, if present, to be above the CMB, as little heterogeneity is expected in the liquid core[12]. The bounce points of the ScP arrivals shown here are interesting for two reasons. First, this region beneath southern Alaska shows clear evidence for an anomalously fast D″ layer from long-period shear waves[13]. The top of the D″ layer is ~250 km above the CMB. We see no evidence of reflections from this height, which may indicate that the transition at the top of D″ is rather gradual. Second, arrivals between P and PcP that are identifiable on individual traces have been interpreted[14] as arising from intermittent layering above the CMB just a few hundred kilometres away from our bounce points, yet we do not see these arrivals on our traces.

The interval before the arrival of ScP from the larger, 13 March earthquake is clean. No coherent energy is visible in the complete seismic section, nor in the numerous sections from subsets of the data that we examined. The noise levels are 5–20% of the ScP amplitude, and in our experience, arrivals as small as one-half of the noise level are visible in such dense record sections. As a more sensitive test for layered reflectors, we aligned the ScP arrivals, then summed the traces. The noise level is near 0.5%. There are no clear short-period reflections from the top nor from within D″.

The sharpness of the CMB may be estimated from the reflection coefficient of ScP as a function of frequency. It is apparent from high-pass filtered traces that 2-Hz energy is reflected from the CMB along our entire profile. And the duration of the 2-Hz arrivals is ~5 s, close to the duration of the earthquake. The presence of 2-Hz reflections shows that the CMB has a significant vertical velocity gradient spanning less than 1 km across the entire profile.

We conclude that within our resolution, the CMB is flat, sharp, lacks lateral variation and is not overlain by structures that would reflect 0.5- to 2-Hz energy, at least for a 350-km span beneath the northeast Pacific Ocean.

The lack of topography greater than 500 m with a scale length of 50–200 km directly confirms inferences drawn from PcP amplitudes[10,11], PKP precursors[15] and length of day fluctuations[16]. The boundary sharpness required along this section of the CMB, with the change from mantle to core occurring across less than 1 km, is more stringent than previous measurements from individual records of P and PcP[5,6].

The lack of overlying structure is in contrast to the results of long-period studies. Long-period shear wave studies worldwide indicate an intermittent 2–5% increase in impedance with depth roughly 250 km above the CMB[17,18]. Near Alaska, at the location of our bounce points, the 2–3% increase in the shear wave velocity has been proposed[19] to occur in a depth range of less than 25 km. The long-period measurements show that the D″ layer is faster than normal mantle[17,20]. This argues against its being interpreted solely as a thermal boundary layer, as a hot D″ would be slow[2]. Our lack of observed short-period reflections requires that such a boundary be broader than 5 km. The absence of critical reflections from the top of D″ also argues for a gradual boundary[21], as mentioned above. A remote possibility is that the boundary is so irregular that short-period energy reflects incoherently, whereas long-period reflections can be observed. Thus, either D″ is absent in the region that we sample, or its upper boundary is unexpectedly diffuse. □

Received 5 June; accepted 28 August 1992.

1. Lay, T. *Eos* **70,** 54–55; 58–59 (1989).
2. Jeanloz, R. & Richter, F. M. *J. geophys. Res.* **84,** 5497–5504 (1979).
3. Williams, Q. & Jeanloz, R. *J. geophys. Res.* **95,** 19299–19310 (1990).
4. Knittle, E. & Jeanloz, R. *Geophys. Res. Lett.* **16,** 609–612 (1989).
5. Kanamori, H. *J. geophys. Res.* **72,** 559–572 (1967).
6. Niazi, M. & McLaughlin K. L. *J. Geodynam.* **8,** 1–16 (1987).
7. Chowdhury, D. K. & Frasier, C. W. *J. geophys. Res.* **78,** 6021–6028 (1973).
8. Vidale, J. E. & Benz, H. M. *Nature* **356,** 678–683 (1992).
9. Burdick, L. J. *Geophys. Jl R. astr. Soc.* **80,** 35–55 (1985).
10. Menke, W. *Geophys. Res. Lett.* **13,** 1501–1504 (1986).
11. Kampfmann, W. & Müller, G. *Geophys. Res. Lett.* **16,** 653–656 (1989).
12. Stevenson, D. *J. Geophys. Jl R. astr. Soc.* **88,** 311–319 (1987).
13. Young, C. J. & Lay, T. *A. Rev. Earth planet. Sci.* **15,** 25–46 (1987).
14. Weber, M. & Koernig, M. *Geophys. Res. Lett.* **17,** 1993–1996 (1990).
15. Bataille, K. & Flatté S. M. *J. geophys. Res.* **93,** 15057–15064 (1990).
16. Gwinn, C. R., Herring, T. A. & Shapiro, I. I. *J. geophys. Res.* **91,** 4755–4767 (1986).
17. Lay, T. & Helmberger, D. V. *J. geophys. Res.* **88,** 8160–8170 (1983).
18. Revenaugh, J. & Jordan, T. H. *J. geophys. Res.* **96,** 19811–19824 (1991).
19. Young, C. J. & Lay, T. *J. geophys. Res.*, **95,** 17385–17402 (1990).
20. Tanimoto, T. *Geophys. J. int.* **100,** 327–336 (1990).
21. Schlittenhardt, J. *J. geophys.* **60,** 1–18 (1986).

ACKNOWLEDGEMENTS. We thank S. Grand, T. Lay and Q. Williams for discussions and H. Houston, C. Ammon, S. Kirby, M. Weber and J. Mori for comments. X. Y. Ding estimated effects of attenuation from reference Earth models. J. Mori removed the instrument response for Fig. 3. R. Crosson demonstrated the effectiveness of source deconvolution. R. Benson and R. Somera assisted in recovering the data.

Blade-shaped conodont elements functioned as cutting teeth

Mark A. Purnell* & Peter H. von Bitter

Department of Invertebrate Palaeontology, Royal Ontario Museum and University of Toronto, 100 Queen's Park, Toronto, Ontario M5S 2C6, Canada

CONODONTS were small eel-shaped animals with vertebrate affinities[1–4]. Known almost exclusively from the small, tooth-like, phosphatic elements of their feeding apparatus, they have one of the finest fossil records of any group of organisms. Until recently the identity of the animal to which conodont elements belonged was one of palaeontology's great mysteries; the function of the elements themselves, particularly blade-shaped elements, remains uncertain (compare refs 3 and 4). But recent insights into the conodont skeletal Bauplan[5] allow the debate over function to be taken beyond arguments of analogy. Here we present a functional analysis of opposed blade-shaped-element pairs as components of an integrated apparatus. From this we conclude that such elements operated as cutting teeth within a grasping and food-processing apparatus.

Much of the debate over the function of conodont elements[6–11] took place before the anatomy of the animal[1,2] and the architecture of the skeletal apparatus[5] were known. Consequently, these analyses were limited by the lack of developmental and structural context for the conodont elements and "the entire field of functional morphology [was] essentially closed to conodont workers"[10]. More recent studies have considered the elements as components of an integrated feeding structure within an eel-shaped animal and two functional models have been proposed. The anterior elements of the conodont apparatus, the S and M elements (Fig. 1), may have functioned together as a ciliated sieve structure that sorted small food particles to be bruised or crushed gently by the posterior Pa and Pb elements[12,13] (Fig. 1). Alternatively, it has been suggested[1,5] that the anterior elements grasped the food, which was then cut and ground by the Pb and Pa elements (Fig. 1).

Some of the most convincing evidence for Pa element function

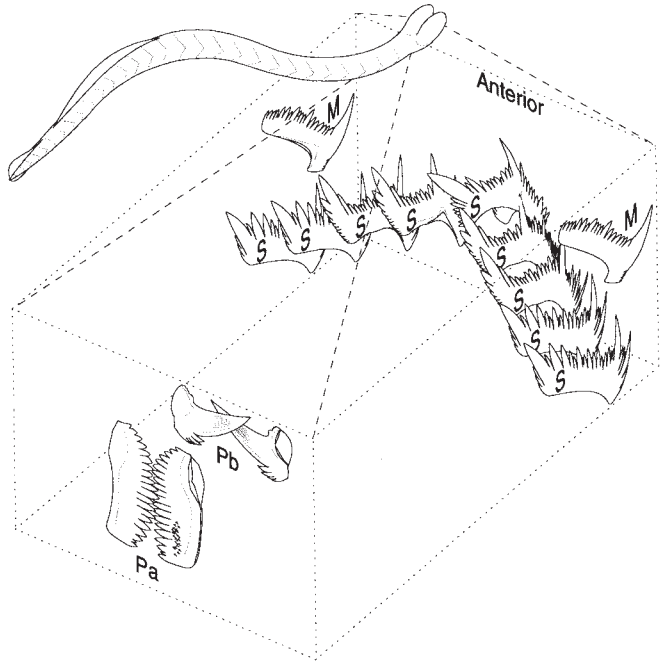

FIG. 1 Feeding apparatus architecture of *Vogelgnathus campbelli* showing the location of the apparatus in the animal. Elements are shown ×45. Relative size is based on bedding plane assemblage specimen 62P-701 (ref. 16). Apparatus architecture is based on ref. 5; S elements are shown more widely spaced than in nature. Animal is shown ~×1.7, morphology is diagrammatic, based on refs 1, 2 and 22.

* Present address: Department of Geology, University of Leicester, University Road, Leicester LE1 7RH, UK.